ISSN 0164-0313, Volume 29, Number 3

J Fusion Energ (2010) 29:223–231
DOI 10.1007/s10894-009-9262-6

ORIGINAL PAPER

Numerical Experiments on Oxygen Soft X-Ray Emissions from Low Energy Plasma Focus Using Lee Model

M. Akel · Sh. Al-Hawat · S. H. Saw · S. Lee

Published online: 22 November 2009

Abstract The X-ray emission properties of oxygen plasmas are numerically investigated using corona plasma equilibrium model. The Lee model is here modified to include oxygen in addition to other gases. It is then applied to characterize the Rico Plasma Focus (1 kJ), finding a oxygen soft X-ray yield (Ysxr) of 0.04 mJ in its typical operation. Keeping the bank parameters and operational voltage unchanged but systematically changing other parameters, numerical experiments were performed finding the optimum combination of pressure = 3 Torr, anode length = 1.5 cm and anode radius = 1.29 cm. The optimum Ysxr was 43 mJ. Thus we expect to increase the oxygen Ysxr of PF-1 kJ thousand-fold from its present typical operation; without changing the capacitor bank, merely by changing the electrode configuration and operating pressure. The modified version of the Lee model code is also used to run numerical experiments with oxygen gas, for optimizing the oxygen soft X-ray yield on the new plasma focus device PF-SY2 (2.8 kJ). The static inductance L_0 of the capacitor bank is progressively reduced to assess the effect on pinch current I_{pinch}. The experiments confirm the I_{pinch}, limitation effect in plasma focus, where there is an optimum L_0 below which although the peak total current, I_{peak}, continues to increase progressively with progressively reduced inductance L_0, the I_{pinch} and consequently the soft X-ray yield, Ysxr, of that plasma focus would not increase, but instead decreases. The obtained results indicate that reducing the present L_0 of the PF-SY2 device will increase the oxygen soft X-ray yield till the maximum value after that the Ysxr will decrease with I_{pinch} decreasing.

Keywords Low energy plasma focus · Soft X-ray · Oxygen gas · Lee Model RADPF5.15 K

M. Akel (✉) · Sh. Al-Hawat
Department of Physics, Atomic Energy Commission, P.O. Box 6091, Damascus, Syria
e-mail: scientific@aec.org.sy

S. H. Saw · S. Lee
Institute for Plasma Focus Studies, 32 Oakpark Drive, Chadstone, VIC 3148, Australia

S. Lee
National Institute of Education, Nanyang Technological University, Singapore 637616, Singapore

S. H. Saw · S. Lee
INTI International University College, 71800 Nilai, Malaysia

Introduction

The dynamics of plasma focus discharges is complicated; for this purpose, to investigate the plasma focus phenomena, the Lee model couples the electrical circuit with plasma focus dynamics, thermodynamics and radiation, enabling realistic simulation of all gross focus properties.

In the radial phases, axial acceleration and ejection of mass are caused by necking curvatures of the pinching current sheath result in time-dependent strongly center-peaked density distributions. Moreover laboratory measurements show that rapid plasma/current disruptions result in localized regions of high densities and temperatures particularly in the heavy gases like xenon. We need to point out that these center-peaking density effects and localized regions are not modeled in the code, which consequently computes only an average uniform density and an average uniform temperature which are considerably lower than measured peak density and temperature. However, because the 4-model parameters are obtained by

fitting the computed total current waveform to the measured total current waveform, the model incorporates the energy and mass balances equivalent, at least in the gross sense, to all the processes which are not even specifically modeled. Hence the computed gross features such as speeds and trajectories and integrated soft X-ray yields have been extensively tested in numerical experiments for several machines and are found to be comparable with measured values.

Thus the code provides a useful tool to conduct scoping studies, as it is not purely a theoretical code, but offers means to conduct phenomenological scaling studies for any plasma focus device from low energy to high energy machines.

The model in its two-phase form was described in 1984 [1]. It was successfully used to assist in the design and interpretation of several experiments [2–6]. Radiation-coupled dynamics was included in the five-phase code leading to numerical experiments on radiation cooling [7]. The vital role of a finite small disturbance speed discussed by Potter [8] in a Z-pinch situation was incorporated together with real gas thermodynamics and radiation-yield terms. Before this 'communication delay effect' was incorporated, the model consistently over-estimated the radial speeds by a factor of ~ 2 and shock temperatures by a factor ~ 4. This version using the 'signal-delay slug' assisted other research projects [9–11] and was web-published in 2000 [12] and 2005 [13]. All subsequent versions of the Lee model code incorporate the 'signal-delay slug' as a must-have feature. Plasma self-absorption was included in 2007 [12] improving soft X-ray yield simulation in neon, argon and xenon among other gases. The model has been used extensively as a complementary facility in several machines, for example, UNU/ICTP PFF [2, 5, 9, 10, 14–17], NX1 [10, 18] NX2 [10, 11] and DENA [19]. It has also been used in other machines for design and interpretation including sub-kJ plasma focus machines [20]. Information obtained from the model includes axial and radial velocities and dynamics [19], dimensions and duration of the focus pinch, gross information of temperatures and densities within the pinch, soft X-ray emission characteristics and yield [10, 11, 21], design and optimization [20, 21], of machines, and adaptation to other machine types such as the Filippov-type DENA [19]. The versatility and utility of the improved model is demonstrated in the clear distinction of pinch current from the peak current [22] and the recent uncovering of a plasma focus pinch current limitation effect [23–26]. The detailed description, theory, latest code and a broad range of results of this 'Universal Plasma Focus Laboratory Facility' are available for download from ref. [27].

Oxygen has been used in plasma focus devices as a rich ion source for material science applications [28, 29]. To characterize the plasma focus device operated in oxygen, in this work the Lee model code was modified to include oxygen gas. For this purpose, the oxygen ionization energy data was extracted from NIST [30], and using the corona-model sub-routines available on the IPFS website [27], thermodynamic data such as ionization curves, effective charge numbers and specific heat ratios for oxygen were calculated. Next, these data were fed into the latest Lee code RADPF5.15 K using the 6-polynomials method for the oxygen thermodynamic data.

This work has progressed the Lee model code to the version RADPF5.15 K, which enables to run numerical experiments with the following gases: hydrogen, deuterium, deuterium-tritium, helium, neon, argon, xenon, krypton, nitrogen and oxygen.

In this paper, the Lee Model RADPF5.15 K was used in numerical experiments on two low energy plasma focus devices: Rico Plasma focus (1 kJ) [28, 29] and PF-SY2 (2.8 kJ) operating with oxygen gas.

Calculations of Oxygen Plasma Parameters Using Corona Model

The X-ray radiation properties of plasma are dependent on the plasma temperature, ionization states and density. Plasma equilibrium model can be used to calculate the ion fraction α, the effective ionic charge number Z_{eff}, the effective specific heat ratio γ and X-ray emission of the plasma at different temperatures.

The corona model [11, 27, 31–33] has been used as an approximation for computing the thermodynamic data of the oxygen plasma in the plasma focus. The data of ionization potentials and X-ray emission spectrum of highly ionized oxygen plasma are taken from NIST [30]. Based on the corona model, the ion fraction, effective ionic charge number and effective specific heat ratio for oxygen plasma have been calculated at different temperatures, for more details see [11, 32]. The obtained results for the ion fraction and effective ionic charge number are shown in Figs. 1, 2.

Looking at the results displayed in Fig. 1, the suitable temperature range for generating H-like 1s-2p, O_2: 18.97 A^o ($h\nu_1 = 653.68$ eV), 1s-3p, O_2: 16 A^o ($h\nu_2 = 774.634$ eV) and He– like $1s^2$-1s2p, O_2: 21.6 A^o ($h\nu_3 = 573.947$ eV), $1s^2$-1s3p, O_2: 18.62 A ($h\nu_4 = 665.615$) ions in oxygen plasma (therefore soft X-ray emissions) is between 119–260 eV (1.38×10^6–3×10^6 K). Also the important feature can be seen from Fig. 2, that the temperatures range 49.44–80.53 eV corresponds to the $1s^2$ close shell for the oxygen ions. Therefore, the yield from X-ray line emissions is low in this temperature range from oxygen. And it can be noticed that the oxygen atoms become fully ionized around 2,000–3,000 eV.

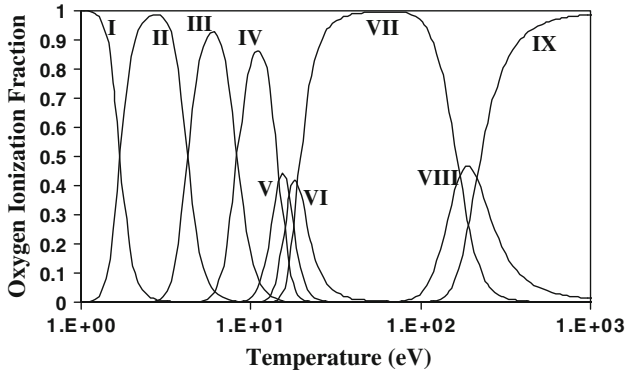

Fig. 1 Oxygen ion fractions at different temperature, where IX indicates the ion O^{+8}

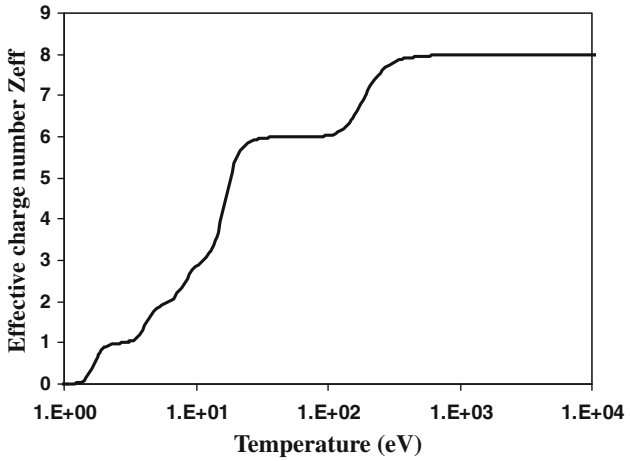

Fig. 2 Effective ionization number Z_{eff} of oxygen (calculated by corona model)

The power of line emissions can also be calculated [11, 32], and the intensities of Lyman—alpha (Ly_α), helium—alpha (He_α) lines are proportional to the H-like and He-like ion densities , respectively. Using the following equations the radiation power of Ly_α, Ly_β and He_α, He_β lines for oxygen as functions of photon energy hν are [11]:

$$P_{Ly\alpha(1s-2p)} = k_1 \cdot N_i^2 \cdot \alpha_7 \cdot Z_{eff} \cdot e^{\left(\frac{-h\nu_1}{T_{ev}}\right)} / \sqrt{T_{eV}} \quad (1)$$

$$P_{Ly\beta(1s-3p)} = k_2 \cdot N_i^2 \cdot \alpha_7 \cdot Z_{eff} \cdot e^{\left(\frac{-h\nu_2}{T_{ev}}\right)} / \sqrt{T_{eV}} \quad (2)$$

$$P_{He\alpha(1s^2-1s2p)} = k_3 \cdot N_i^2 \cdot \alpha_6 \cdot Z_{eff} \cdot e^{\left(\frac{-h\nu_3}{T_{ev}}\right)} / \sqrt{T_{eV}} \quad (3)$$

$$P_{He\beta(1s^2-1s3p)} = k_4 \cdot N_i^2 \cdot \alpha_6 \cdot Z_{eff} \cdot e^{\left(\frac{-h\nu_4}{T_{ev}}\right)} / \sqrt{T_{eV}} \quad (4)$$

where: $k_1 = 2 \times 10^{-31}$, $k_2 = 4 \times 10^{-32}$, $k_3 = 1.3 \times 10^{-31}$, $k_4 = 3 \times 10^{-32}$.From these equations it can be seen that the radiation power is proportional to the density squared, ion fraction and Z_{eff}. Then the normalized emission intensity can be calculated by putting $N_i = 1$. The calculated Ly and He emission intensities from one oxygen ion at unit density are given in Fig. 3. The related ion fractions are also plotted in this figure, which clearly shows the relationship between the line emission intensity with corresponding ions. The peaks of the Ly and He lines are located at the higher temperature side of the H-like and He-like ion distributions. It means the ions need to be heated to excited states to give X-ray emissions. The locations of the peaks give us a rough knowledge of the optimum temperatures for generating X-rays from oxygen plasma, i.e. 225 eV. Choice of optimum temperature is made in comparison with the optimum temperatures chosen for nitrogen [33], neon and argon in Shan Bing's work [11]. The comparison is shown in Table 1. It can be seen that much more energy is required to heat the argon to its X-ray optimum temperature. Hence the usual method for increasing the plasma temperature (by increase the energy density) is to decrease the filling gas pressure. However, the X-ray yield is also related to the total number of X-ray emitters which is proportional to the gas pressure. Therefore, the optimum oxygen X-ray yield temperature may be lower than 260 eV in a plasma focus.

X-Ray Emissions in Plasma Focus and its Incorporation in Model Code

The focused plasma, with electron temperature of a few hundreds eV to about keV and high enough electron density, is a copious source of X-rays. The plasma focus emits both soft (thermal) as well as hard (non-thermal) X-rays but for the scope of this paper we will concentrate only on soft thermal X-rays. The plasma focus emits soft thermal X-rays by three processes [34, 35], namely: Bremsstrahlung (free-free transition) from the coulomb interactions between electrons and ions; recombination radiation (free-bound transition) emitted by an initially free electron as it

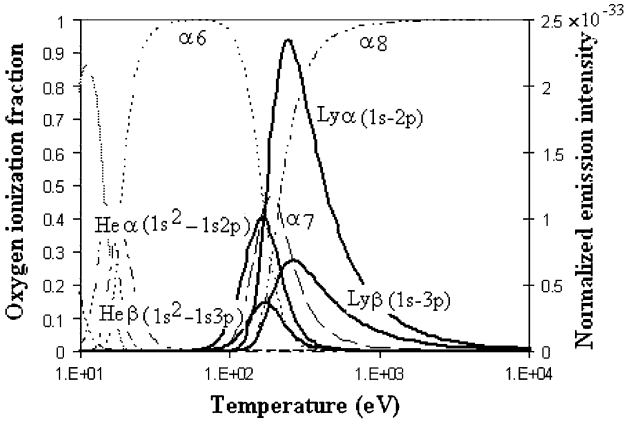

Fig. 3 Calculated X-ray line emission intensities from oxygen Ly and He lines vs temperature. The *dot lines* are the ions fractions (calculated by corona model)

Table 1 Optimization conditions for X-ray radiative plasma of Oxygen, Nitrogen, Neon and Argon

Gas	Temperature	Z_{eff}	$E_{ion} = E_i + (3/2)(1 + Z_{eff})kT$
Oxygen	~225 eV	7.38	1.59 + 2.82 keV
Nitrogen	~160 eV	6.48	1.16 + 1.79 keV [33]
Neon	~420 eV	9.38	2.69 + 4.36 keV [11]
Argon	~3 keV	17.00	11.03 + 54 keV [11]

loses energy on recombination with an ion; and de-excitation radiation (bound-bound transition) when a bound electron loses energy by falling to a lower ionic energy state. The first two processes give rise to the continuum of the X-ray spectrum while the third process produces the characteristic line radiation of the plasma. The relative strengths of the continuum and line emissions depend on how the plasma was formed; typically, for plasma formed from a high-Z material continuum emission dominates, while for a low-Z material line emission can be stronger. The calculation of the power emitted by processes within the plasma depends on assumptions made about the state of the plasma.In the code [27, 36–38] in pinch phase, line radiation Q_L is calculated using the relation

$$\frac{dQ_L}{dt} = -4.6 \times 10^{-31} N_i^2 Z_{eff} Z_n^4 (\pi a_{min}^2) Z_{max}/T \quad (5)$$

after being integrated over the pinch duration. Hence the soft X-ray energy generated within the plasma pinch depends on the properties: number density N_i, effective charge number Z_{eff}, atomic number of gas Z_n, pinch radius a_{min}, pinch length Z_{max}, plasma temperature T and the pinch duration. This generated energy is then reduced by the plasma self-absorption which depends primarily on density and temperature; the reduced quantity of energy is then emitted as the soft X-ray yield.

Based on the corona model, in the code we take the oxygen soft X-ray yield (generation H-like and He-like ions) to be equivalent to line radiation yield i.e. $Y_{sxr} = Q_L$ at the following temperature range 119–260 eV.

Procedures for Numerical Experiments Using RADPF5.15 K

The Lee code is configured to work as any plasma focus by inputting the bank parameters, the tube parameters, operational parameters and the fill gas. The standard practice is to fit the computed total current waveform to an experimentally measured total current waveform using four model parameters representing the mass swept-up factor f_m, the plasma current factor f_c for the axial phase and factors f_{mr} and f_{cr} for the radial phase.

The axial and radial phase dynamics and the crucial energy transfer into the focus pinch are among the important information that is quickly apparent from the current trace. The exact time profile of the total current trace is governed by the bank parameters, by the focus tube geometry and the operational parameters. It also depends on the fraction of the mass swept up and the fraction of sheath current and the variation of these fractions through the axial and radial phases. These parameters determine the axial and radial dynamics, specifically the axial and radial speeds which in turn affect the profile and magnitudes of the discharge current. The detailed profile of the discharge current during the pinch phase also reflects the Joule heating and radiative yields. At the end of the pinch phase the total current profile also reflects the sudden transition of the current flow from a constricted pinch to a large column flow. Thus, the discharge current powers all dynamic, electrodynamic, thermodynamic and radiation processes in the various phases of the plasma focus. Conversely all the dynamic, electrodynamic, thermodynamic and radiation processes in the various phases of the plasma focus affect the discharge current. It is then no exaggeration to say that the discharge current waveform contains information on all the dynamic, electrodynamic, thermodynamic and radiation processes that occur in the various phases of the plasma focus. This explains the importance attached to matching the computed current trace to the measured current trace in the procedure adopted by the Lee model code [12, 13, 22–24, 39, 40].

The numerical experiments for soft X-ray optimization from oxygen plasma were investigated on two low energy plasma focus devices: Rico Plasma focus (1 kJ) and PF-SY2.

PF-1 kJ-:The Numerical Experiments

The Rico Plasma focus (1 kJ) [28, 29] operated with oxygen filling gas at the following bank and tube parameters:

Bank parameters: $L_0 = 65$ nH, $C_0 = 3.86$ μF, $r_0 = 22$ mΩ,
Tube parameters: $a = 1.75$ cm, $b = 4.9$ cm, $z_0 = 6.75$ cm,
Operating parameters: $V_0 = 14.9$ kV, $p_0 = 0.2$ Torr, oxygen gas,

where L_0 is the static inductance (nominal), C_0 the storage capacitance (nominal), b the tube outer radius, a the inner radius, z_0 the anode length, V_0 the operating voltage and p_0 the operating initial pressure. The measured current derivative waveform at the above conditions is shown in Fig. 4.

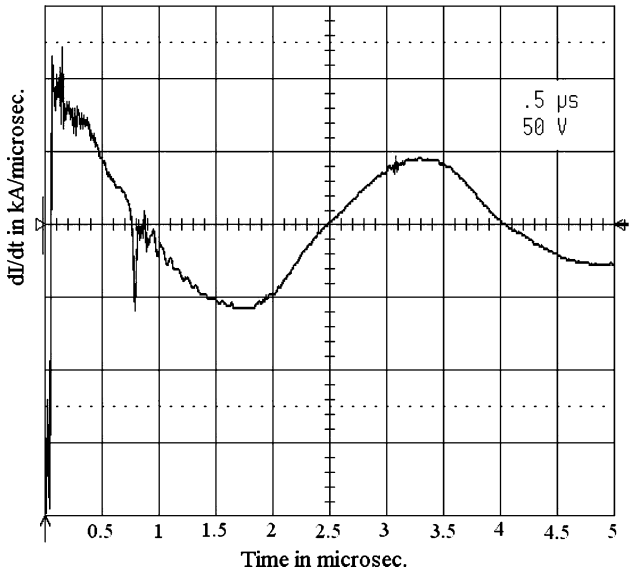

Fig. 4 The temporal evolution of derivative current of the oxygen discharge during the plasma focus formation in PF-1 kJ. $V_0 = 14.9$ kV, $p_0 = 0.2$ Torr, $C_0 = 3.86$ μF, $L_0 = 65$ nH, $r_0 = 22$ mΩ

We first digitize the measured current derivative waveform using an open access source digitizing program, Engauge [41] and then integrate the data with time to obtain the current waveform. Then we fit the computed current waveform to the measured waveform as follows:

We configure the Lee model code (version RADPF5.15 K) to operate as the Rico Plasma focus (1 kJ) starting with the above bank and tube parameters.

To obtain a reasonably good fit the following parameters are used:

Bank parameters: $L_0 = 69$ nH, $C_0 = 3.86$ μF, $r_0 = 20$ mΩ,
Tube parameters: $b = 4.9$ cm, $a = 1.75$ cm, $z_0 = 6.75$ cm,
Operating parameters: $V_0 = 14.9$ kV, $p_0 = 0.2$ Torr, oxygen gas,

together with the following fitted model parameters:
$f_m = 0.004$, $f_c = 0.7$, $f_{mr} = 0.015$ and $f_{cr} = 0.45$.

It can be seen that the computed discharge current waveform agrees well with the measured current waveform up to and slightly beyond the bottom of the current dip (Fig. 5). This means that the agreement covers all the regions of interest from axial to radial phases up to the end of the pinch phase; all five plasma focus phases of interest to us.

The numerical experiments using RADPF5.15 K at the bank and tube parameters last mentioned above and using the fitted model parameters give then the following results: the end axial speed to be $V_a = 17.6$ cm/μs, the final plasma column is 0.19 cm in radius, and 2.1 cm in length.

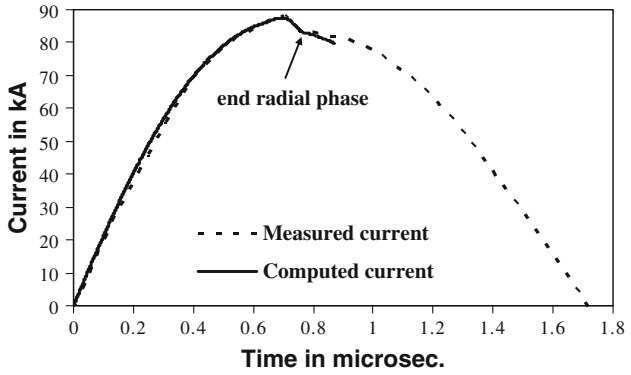

Fig. 5 Comparison of the computed current trace (*solid smooth line*) with the experimental one (*dotted line*) of the PF- 1 kJ at 14.9 kV, 0.2 Torr at oxygen filling gas

Also the Ysxr emitted from the oxygen plasma is calculated at the above conditions, to be 0.04 mJ (see Table 2). Form Table 2 at $p_0 = 0.2$ Torr, it can be found, that the axial speed is very high, and consequently the temperature will be higher than suitable for soft X-ray generation. This low soft X-ray yield from Rico Plasma focus (1 kJ) at experimental conditions is already expected, since Rico Plasma focus (1 kJ) was modified to use as ion beam source for material science applications, and not to generate soft X-ray or line radiation.

As the first step, the code RADPF5.15 K was run to optimize X-ray yield from PF-1 kJ with oxygen gas as function of only pressure; fixing all the mentioned above parameters. The pressure was varied from 0.2 to 0.9 Torr.

As is well known, when the operating pressure is increased, the plasma speeds decrease; hence, the duration of the axial phase increases. From Table 2 it is seen that the Ysxr increases with increasing pressure until it reaches the maximum value about 6.8 mJ at $p_0 = 0.745$ Torr, after which it decreases with higher pressures. As expected as p_0 is increased, the end axial speed, the inward shock speed and the radial piston speed all reduced. The decrease in speeds lead to lowering of plasma temperatures below that needed for soft X-ray production. From Table 2 we note that a shift of operating pressure to 0.745 Torr would increase the computed Ysxr to 6.8 mJ.

To optimize the soft X-ray yield from Rico Plasma focus (1 kJ) with oxygen gas, more numerical experiments were carried out with the above model parameters; but varying p_0, z_0 and 'a' keeping $c = b/a$ constant at value $c = 2.8$. The pressure p_0 was varied from 1 to 15 Torr.

The following procedure was used [33]:

- At each p_0, the anode length z_0 was fixed at a certain value,
- Then the anode radius 'a' was smoothly varied, till the maximum X-ray yield (Ysxr) was obtained for this certain value of z_0.

Table 2 Variation PF-1 kJ parameters with pressure at: $L_0 = 69$ nH, $C_0 = 3.86$ μF, $r_0 = 20$ mΩ, $V_0 = 14.9$ kV, RESF = 0.150, c = b/a = 2.8, $f_m = 0.004$, $f_c = 0.7$, $f_{mr} = 0.015$, $f_{cr} = 0.45$, oxygen gas

p_0 (Torr)	I_{peak} (kA)	I_{pinch} (kA)	V_a (cm/μs)	V_s (cm/μs)	V_p (cm/μs)	Pinch dur. (ns)	T_{pinch} (10^6 K)	Ysxr (mJ)
0.2	87	38	17.6	35.3	24.4	12.7	8.39	0.04
0.3	89	38	15.2	29.8	20.9	14.8	5.62	0.16
0.5	91	35	12.4	22.8	16.3	19.2	2.94	1.2
0.7	92	30	10.6	17.9	13.1	24.9	1.60	5.1
0.72	92	30	10.5	17.5	12.8	25.6	1.50	5.7
0.73	92	29	10.4	17.2	12.7	25.9	1.45	6.1
0.74	92	29	10.4	17.0	12.5	26.2	1.41	6.5
0.745	92	29	10.3	16.9	12.5	26.5	1.38	6.8
0.75	92	29	10.3	16.8	12.4	26.7	1.36	6
0.77	93	28	10.2	16.4	12.1	27.6	1.27	2
0.8	93	27	10.0	15.8	11.7	28.9	1.14	0
0.9	93	24	9.4	13.8	10.4	34.5	0.78	0

- After that, we chose another value of z_0, varying the value of 'a' looking for the maximum of Ysxr, until we found the optimum combination of z_0 and 'a' for the best X-ray yield at the fixed p_0.
- Then we changed p_0 and repeated the above procedure to find the optimum combination of z_0 and 'a' corresponding to this new value of p_0. We proceed until we had obtained the optimum combination of p_0, z_0 and 'a' for the maximum soft X-ray yield.

For optimum oxygen Ysxr, as mentioned earlier, there is an optimum temperature. This implies that there is an optimum speed factor [6] $S = (I_{peak}/a)/p_0^{0.5}$. As p_0 was increased in order to maintain the optimum S, (I_{peak}/a) had to be correspondingly increased, by a reduction of 'a'. The numerical experiments also showed that z_0 needed to be increased to optimize the Ysxr (see Table 3). Thus whilst external inductance L_0 is fixed at a constant value and an axial section inductance L_a is increased due to increasing the anode length, the pinch inductance L_p is reduced due to decreasing the pinch length [6, 23].

The optimized results for each value of p_0 are shown in table 3. The table shows that as p_0 is increased, anode length z_0 rises and inner radius 'a' decreases with each increase in p_0, while the soft X-ray yield slightly increases with increasing p_0 until it reaches a maximum value of 43 mJ at $p_0 = 3$ Torr; then the Ysxr decreases with further pressure increase.

Nevertheless the numerical experiments have shown that with the present capacitor bank, Rico Plasma focus (1 kJ) can be improved from its present computed Ysxr of 0.04 mJ corresponding to the yield with its present geometry and usual operating pressure. The optimum geometry requires making the anode length and the anode radius shorter, at the same time increasing its operational pressure.

PF-SY2 (2.8 kJ)-The Numerical Experiments

The numerical experiments were investigated using the parameters of the low energy plasma focus PF-SY2 and optimizing for a X-ray source. The bank parameters were $L_0 = 200$ nH, $C_0 = 25$ μF and $r_0 = 14$ mΩ. The tube parameters were the outer radius b = 3.2 cm, the inner radius a = 0.95 cm, and the anode length $z_0 = 16$ cm. The operating parameters were $V_0 = 15$ kV, and $p_0 = 10$ Torr, filling oxygen gas. The above mentioned parameters were put into the code RADPF5.15 K.

Table 3 X-ray yield optimization from PF-1 kJ for each value of p_0 varying z_0 and 'a' at filling oxygen gas

p_0 (Torr)	z_0 (cm)	a (cm)	I_{peak} (kA)	I_{pinch} (kA)	Ysxr (mJ)	V_a (cm/μs)	a_{min} (cm)	z_{max} (cm)
1.0	1.0	2.18	92	40	41	4.8	0.20	2.7
2.0	1.3	1.57	92	41	42	5.3	0.14	1.9
3.0	1.5	1.29	92	41	43	5.6	0.12	1.6
5.0	1.8	1.01	93	41	42	5.9	0.09	1.2
10.0	2.8	0.71	95	42	37	6.7	0.07	0.9
15.0	3.0	0.58	95	42	33	6.8	0.05	0.7

$L_0 = 69$ nH, $C_0 = 3.86$ μF, $r_0 = 20$ mΩ, $V_0 = 14.9$ kV, RESF = 0.150, c = b/a = 2.8, $f_m = 0.004$, $f_c = 0.7$, $f_{mr} = 0.015$, $f_{cr} = 0.45$

In this work we would like to present the Mather-type plasma focus device PF-SY2 as a X-ray source with oxygen filling gas using Lee model RADPF5.15 K.

The numerical experiments were conducted using a constant value of a factor RESF = 0.157 (RESF = stray resistance/surge impedance), where at each L_0 the corresponding resistance value was found. Also at each L_0 the ratio (c = b/a) was kept constant at value c = 3.368.

To optimize the soft X-ray yield from PF-SY2 with oxygen gas, varying L_0, z_0 and 'a' keeping 'c' and RESF constant. The external inductance L_0 was varied from 200 to 1 nH.

As we haven't any oxygen measured current trace from PF-SY2, the numerical experiments for optimization soft X-ray from oxygen plasma were carried out with the two different model parameters:

The first model parameters: $f_m = 0.05$, $f_c = 0.7$, $f_{mr} = 0.1$, and $f_{cr} = 0.7$,
The second model parameters: $f_m = 0.03$, $f_c = 0.7$, $f_{mr} = 0.08$, and $f_{cr} = 0.7$.

The following procedures were used:

At each L_0, the pressure was fixed at constant value (in our case $p_0 = 10$ Torr) and also the anode length was fixed at a certain value:

- Then the inner radius 'a' was varied, whilst keeping c = 3.368, until the maximum X-ray yield was obtained for this certain value of z_0.
- After that we chose another value of z_0, varying 'a' until maximum X-ray yield and so on, until we have obtained the combination of z_0 and 'a' for the best maximum X-ray yield at a fixed L_0 (Ysxr vs z_0 and 'a' at fixed L_0 and p_0).
- We repeated the above procedure for progressively smaller L_0 until $L_0 = 1$ nH.

At each L_0, after z_0 was varied, the inner radius 'a' was adjusted to obtain the optimum X-ray yield, which we find to correspond closely to the largest I_{pinch}.

The soft X-ray optimization for each value of L_0, varying z_0 and 'a' is shown in Tables 4, 5. The tables show that as L_0 is reduced, I_{peak} increases with each reduction in L_0 with no sign of any limitation as function of L_0. However, I_{pinch} reaches a maximum value at $L_0 = 5$ nH, then it decreases with each reduction in L_0, but the ratio I_{pinch}/I_{peak} drops progressively as L_0 decreases. Thus I_{peak} does not show any limitation as L_0 is progressively reduced. However, I_{pinch} has a maximum value. This pinch current limitation effect is not a simple, but it is a combination of the two complex effects: the interplay of the various inductances involved in the plasma focus processes abetted by the increasing coupling of C_0 to the inductive energetic processes, as L_0 is reduced [23, 25].

From Tables 4, 5 it can be seen, that as L_0 is decreased, the soft X-ray yield increases until it reaches a maximum value of 10 J at $L_0 = 5$ nH (where I_{pinch} also has maximum); beyond which the soft X-ray yield does not increase with reducing L_0. Thus with decreasing L_0 the pinch current I_{pinch} and the soft X-ray yield show limitation. The obtained results confirm the pinch current limitation effect in oxygen plasma focus, and consequently the soft X-ray yield. Figures 6, 7 represent I_{pinch} and X-ray limitation effects in oxygen plasma focus at 10 Torr as L_0 is reduced from 200 to 1 nH.

Looking at Tables 4 and 5, it is noticed that as L_0 was progressively reduced, to optimize 'a' had to be progressively increased and z_0 progressively decreased. Also the plasma pinch dimensions (pinch radius a_{min} and pinch length Z_{max}) increased as L_0 was reduced.

As the external inductance L_0 is lowered from 200 to 1 nH, the tube inductance ($L_a = 2\times10^{-7}$ ln (b/a) Z_0) is decreased and the focus pinch inductance ($L_p = \sim$ln (b/a_{min}) Z_{max}) is increased [23, 39].

Based on the obtained results of these sets of numerical experiments on PF-SY2 with oxygen gas, we can say that to improve the soft X-ray yield, L_0 should be reduced to a value around 10–15 nH (which is an achievable range incorporating low inductance technology [10]), below which the pinch current I_{pinch} and the soft X-ray yield Ysxr would not be improved much, if at all. These experiments confirm the pinch current limitation effect, and consequently the soft X-ray yield for the oxygen plasma focus. Finally, we would like to emphasize that we, practically, have no intention (or ambition) to go below 10–15 nH (which is an achievable range), but in our numerical experiments using RADPF5.15 K we go down to low values (5–1 nH) just to find the pinch current limitation effect.

Conclusions

The required oxygen plasma thermodynamic parameters (the ion fraction, effective ionic charge number and effective specific heat ratio) were calculated at different temperatures and the X-ray emission properties of oxygen plasma were investigated using corona model.

The Lee model RADPF5.15a was modified to get RADPF5.15 K which includes oxygen gas and it was used to characterize the Rico Plasma focus (1 kJ) using its experimental parameters. The soft X-ray yield was found to be 0.04 mJ at the usual operating pressure $p_0 = 0.2$ Torr. By changing p_0 to 0.745 Torr the Ysxr will increase to 6.8 mJ, as the optimum value for Rico Plasma focus (1 kJ).

The optimum combination of p_0, z_0 and 'a' for optimum soft X-ray yield was found to be: $p_0 = 3$ Torr, $z_0 = 1.5$ cm, a = 1.29 cm and Ysxr = 43 mJ. From these

Table 4 For each L_0 the optimization combination of z_0 and 'a' were found and are listed here

L_0 (nH)	z_0 (cm)	a (cm)	b (cm)	I_{peak} (kA)	I_{pinch} (kA)	I_{pinch} /I_{peak}	a_{min} (cm)	Z_{max} (cm)	Ysxr (J)
200.0	6.1	0.5900	2.0	143	99	0.692	0.06	0.8	0.36
100.0	4.5	0.7700	2.6	198	134	0.676	0.07	1.0	1.03
50.0	3.2	0.9900	3.3	271	175	0.645	0.09	1.4	2.64
40.0	2.8	1.1000	3.7	300	189	0.63	0.11	1.5	3.27
25.0	2.5	1.2000	4.0	365	215	0.589	0.12	1.7	5.52
15.0	2.1	1.3000	4.4	443	237	0.534	0.14	1.8	7.75
10.0	1.7	1.4000	4.7	510	247	0.484	0.17	2.0	9.44
5.0	1.6	1.4600	4.9	627	249	0.397	0.21	2.1	10.06
3.0	1.6	1.4500	4.9	699	244	0.349	0.23	2.1	9.45
1.0	1.6	1.3600	4.6	799	230	0.288	0.234	2.0	7.47

PF-SY2: Bank parameters: $L_0 = 200$ nH, $C_0 = 25$ μF, $r_0 = 14$ mΩ; tube parameter: $c = b/a = 3.368$; model parameters: $f_m = 0.05$, $f_c = 0.7$, $f_{mr} = 0.1$, $f_{cr} = 0.7$; operating at 10 Torr oxygen gas, $V_0 = 15$ kV

Table 5 For each L_0 the optimization combination of z_0 and 'a' were found and are listed here

L_0 (nH)	z_0 (cm)	a (cm)	b (cm)	I_{peak} (kA)	I_{pinch} (kA)	I_{pinch} /I_{peak}	a_{min} (cm)	Z_{max} (cm)	Ysxr (J)
200.0	6.1	0.6700	2.3	141	98	0.695	0.06	0.9	0.43
100.0	4.7	0.8800	3.0	196	133	0.678	0.08	1.2	1.22
50.0	3.2	1.1000	3.7	265	172	0.649	0.10	1.5	3.02
40.0	3.0	1.2000	4.0	293	185	0.631	0.11	1.6	3.91
25.0	2.5	1.4000	4.7	358	209	0.583	0.14	1.9	5.90
15.0	2.1	1.5000	5.1	432	228	0.527	0.17	2.1	8.65
10.0	1.7	1.6000	5.4	494	236	0.477	0.20	2.24	9.97
5.0	1.4	1.6100	5.4	595	239	0.401	0.23	2.29	10.81
3.0	1.2	1.5700	5.3	656	234	0.356	0.24	2.26	9.87
1.0	1.2	1.4600	4.9	741	219	0.295	0.25	2.1	7.22

PF-SY2: Bank parameters: $L_0 = 200$ nH, $C_0 = 25$ μF, $r_0 = 14$ mΩ; tube parameter: $c = b/a = 3.368$; model parameters: $f_m = 0.03$, $f_c = 0.7$, $f_{mr} = 0.08$, $f_{cr} = 0.7$; operating at 10 Torr oxygen gas, $V_0 = 15$ kV

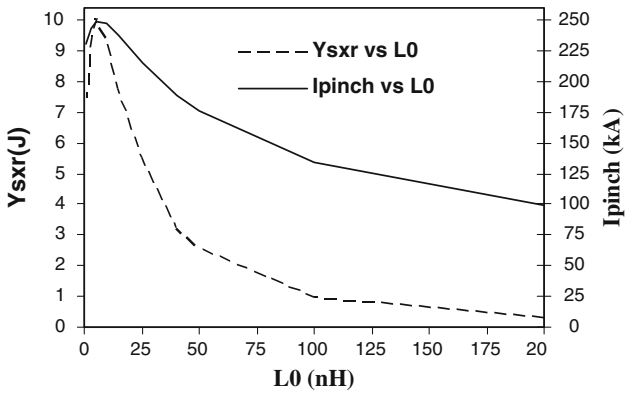

Fig. 6 The X-ray yield from PF-SY2 and I_{pinch} (computed) vs L_0 (200 to 1 nH), model parameters: $f_m = 0.05$, $f_c = 0.7$, $f_{mr} = 0.1$, $f_{cr} = 0.7$; operating at 10 Torr oxygen gas, $V_0 = 15$ kV

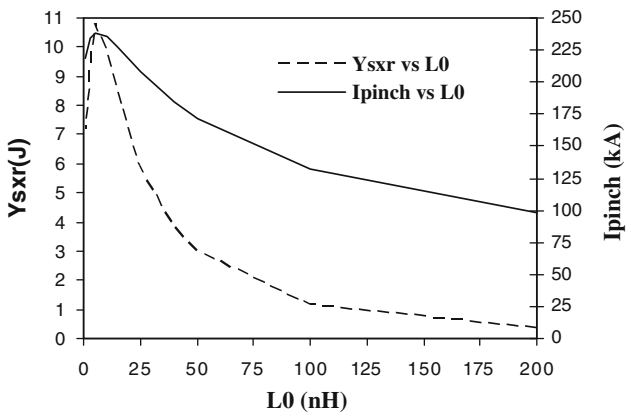

Fig. 7 The X-ray yield from PF-SY2 and I_{pinch} (computed) vs L_0 (200 to 1 nH), model parameters: $f_m = 0.03$, $f_c = 0.7$, $f_{mr} = 0.08$, $f_{cr} = 0.7$; operating at 10 Torr oxygen gas, $V_0 = 15$ kV

numerical experiments we expect to increase the oxygen Ysxr of PF-1 kJ thousand-fold from its present typical operation or hundred-fold from its pressure–optimized present configuration; without changing its capacitor bank, merely by changing its electrode configuration and operating pressure.

The Lee model code RADPF5-15 K was also used to run numerical experiments on PF-SY2 with oxygen gas for optimizing soft X-ray yield with reducing L_0, varying z_0 and 'a'. Contrary to the general expectation that performance of a plasma focus would progressively improve with progressive reduction of its external inductance L_0, the pinch current limitation effect in plasma focus was confirmed with reducing L_0, and consequently the maximum soft X-ray yield was computed as 10 J at $L_0 = 5$ nH; operating the inductance-reduced PF-SY2 at 15 kV, 10 Torr oxygen pressure.

From these numerical experiments we expect to increase the oxygen Ysxr of PF-SY2 with reducing L_0, from the present 0.4 J at $L_0 = 200$ nH to maximum value of near 8 J at an achievable $L_0 = 15$ nH. Because of the current limitation effect, there is little to gain to try to reduce L_0 to 5 nH (which is technically very difficult); and even a loss to reduce L_0 below 5 nH.

Acknowledgments The authors would like to thank Director General of AECS, for encouragement and permanent support. The authors express thanks and appreciation to Dr. L. Rico (Instituto de Fı'sica Rosario (CONICET-UNR), Bvrd. 27 de Febrero 210 Bis, S2000EZP Rosario, Argentina) who provided the Rico Plasma focus (1 kJ) parameters and the measured derivative current waveform of the plasma focus operating with oxygen filling gas. M. Akel would also like to express thanks to Mrs. Sheren Isamael, who collaborated going through all the numerical experiments using Lee Model.

References

1. S. Lee, in *Radiations in Plasmas*, ed. by B. McNamara (World Scientific, Singapore, 1984), pp. 978–987
2. S. Lee et al., Am. J. Phys. **56**, 62 (1988)
3. T.Y. Tou, S. Lee, K.H. Kwek, IEEE Trans. Plasma Sci. **17**, 311 (1989)
4. S. Lee, IEEE Trans. Plasma Sci. **19**, 912 (1991)
5. A. Serban, S. Lee, J. Plasma Phys. **60**, 3–15 (1998)
6. S. Lee, A. Serban, IEEE Trans. Plasma. Sci. **24**, 1101–1105 (1996)
7. J.B. Ali, Development and studies of a small plasma focus PhD thesis, University Technology Malaysia, Kuala Lumpur, Malaysia, 1990
8. D.E. Potter, Nucl. Fusion **18**(6), 813–823 (1978)
9. M.H. Liu et al., IEEE Trans. Plasma. Sci. **26**, 135–140 (1998)
10. S. Lee et al., IEEE Trans. Plasma. Sci. **26**, 1119–1126 (1998)
11. S. Bing, Plasma dynamics and X-ray emission of the plasma focus, PhD thesis NIE ICTP Open Access Archive: http://eprints.ictp.it/99/, 2000
12. S. Lee, http://ckplee.myplace.nie.edu.sg/plasmaphysics/, (2000–2009)
13. S. Lee, ICTP Open Access Archive: http://eprints.ictp.it/85/13, (2005)
14. S. Lee, Twelve years of UNU/ICTP PFF—A Review IC, 98 (231) ICTP, Miramare, Trieste; ICTP OAA: http://eprints.ictp.it/31/, (1998)
15. S.V. Springham et al., Plasma Phys. Control Fusion **42**, 1023–1032 (2000)
16. A. Patran et al., Plasma Sources Sci. Technol. **14**(3), 549–560 (2005)
17. M.A. Mohammadi, S. Sobhanian, C.S. Wong, S. Lee, P.Lee and R.S. Rawat, J. Phys. D: Appl. Phys. **42**, 045203 (2009)
18. E.P. Bogolyubov et al., Phys. Scripta. **57**, 488–494 (1998)
19. V. Siahpoush et al., Plasma Phys. Control Fusion **47**, 1065 (2005)
20. L. Soto et al., Braz. J. Phys. **34**, 1814 (2004)
21. D. Wong et al., Plasma Sources Sci. Technol. **16**, 116–123 (2007)
22. S. Lee et al., Appl. Phys. Lett. **92** 111501 (2008)
23. S. Lee et al., Appl. Phys. Lett. **92** 021503 (2008)
24. S. Lee et al., Plasma Phys. Control Fusion **50** 065012 (2008)
25. S. Lee and S.H. Saw, Appl. Phys. Lett. **94** 076102, (2009)
26. M. Akel, Sh. Al-Hawat, S. Lee, J. Fusion Energ. (2009). doi: 10.1007/s10894-009-9238-6, published online 21 Aug
27. S. Lee, Radiative Dense Plasma Focus Computation Package: RADPF, http://www.intimal.edu.my/school/fas/UFLF/. http://www.plasmafocus.net/IPFS/modelpackage/File1RADPF.htm. (October 2009)
28. L. Rico, B.J. Gomez, J.N. Feugeas, O.de Sanctis, Appl. Surf. Sci. **254**, 193–196 (2007)
29. L. Rico, B.J. Gomez, M. Stachoitti, N. Pellegri, J.N. Feugeas, O.de Sanctis, Braz. J. Phys. **36**(3), 1009–1012 (2006)
30. http://physics.nist.gov/ NIST Atomic Spectra Database Levels Data, (September 2009)
31. S. Lee, Aust. J. Phys. **36**, 891 (1983)
32. M.H. Liu, Soft X-ray from compact plasma focus. PhD thesis, School of Science, Nanyang Technological University, December 1996
33. M. Akel, Sh. Al-Hawat, S. Lee, J. Fusion Energ. **28**(4), 355–363 (2009)
34. E.H. Beckner, J. Appl. Phys. **37**, 4944 (1966)
35. W.H. Bostic, V. Nardi, W. Prior, J. Plasma Phys. **8**, 1 (1972)
36. S.H. Al-Hawat, S. Saloum, Contrib. Plasma Phys. **49**(2), 5–14 (2009)
37. S.H. Saw et al., IEEE Trans. Plasma Sci. **37**(7), 1276–1282 (2009)
38. S. Lee et al., Plasma Phys. Control. Fusion **51**, 105013 (2009)
39. S. Lee, Plasma Phys. Control Fusion **50**, 105005 (2008)
40. S. Lee et al., J. Fusion Energ. **27**(4), 292 (2008)
41. http://sourceforge.net/project/showfiles.php?groupid=67696&package id=130007&release id=500277, (2009)